JOURNAL OF AIRCRAFT
Vol. 47, No. 6, November–December 2010

Engineering Notes

Gauss Pseudospectral Method for Less Noise and Fuel Consumption from Aircraft Operations

M. Houacine* and S. Khardi†
French National Institute for Transport and Safety Research, 69675 Bron, France

DOI: 10.2514/1.C031007

Nomenclature

C_L, C_D	=	lift and drag coefficients
c	=	speed of sound
g	=	gravitational acceleration
m	=	aircraft mass
q	=	dynamic pressure
S	=	reference wing area
T, L, D	=	thrust, lift, and drag forces
t, X, U	=	time, state, and control variables
V_j	=	jet velocity
v	=	aircraft aerodynamic speed
x, y, h	=	Cartesian coordinates
α	=	angle of incidence
δ_x	=	throttle
γ, χ, ϕ	=	flight-path, heading, and roll angles
ρ	=	density of air

I. Introduction

AIR transport has continuously grown over time. The aircraft industry forecasts this growth to be approximately 5% per annum over the next 20 years [1]. If realized, these forecasts would see passengers and cargo traffic increase, respectively, by 180 and 220% between 2007 and 2026 [2]. This rapid growth provides economic benefits and allows a greater mobility of populations. Nevertheless, this increase contributes to green house gas, pollutant emissions and noise annoyance at local level. Intolerance of communities toward disturbances, and the growing proximity of neighborhood areas to aircraft flight paths represents significant constraints to this growth.

In response to concerns of exposed populations, modern aircraft are required to adhere to noise regulations specified in Federal Aviation Regulations FAR 36 [3] and International Civil Aviation Organization (ICAO) Annex 16 [4]. Additionally, it is becoming more common for airports to have their own increasingly stringent noise rules and operational restrictions. Low-noise operational procedures provide operators a way to respond quickly to noise concerns [5].

In this Note, we use a flight parameters optimization approach in order to reduce noise footprints and fuel consumption during approach and takeoff. We start by describing the mathematical model, which is considered as an optimal control problem. Technical feasibility, passenger comfort, and flight safety constraints have been considered. Afterward, we give a brief presentation of the Stone jet noise model [6] and a method to calculate accurately the jet parameters [7] based on the engine inlet and outlet conditions. A Gauss pseudospectral method [8] is proposed to solve the obtained optimal control problem. Some simulation results are given and discussed.

II. Problem Modeling and Analysis

A. Flight Dynamics

Let us start by some assumptions and frames of work.

1) The motion of the point mass aircraft is described in an inertial frame attached to the Earth. Earth is considered as static and flat.

2) The wind effects are not taken into account.

3) The aircraft is considered as a perfect symmetrical rigid object and uniformly mass distributed. Turns are absent in approach and takeoff phases. Therefore, momentum forces are neglected, since all external forces cross the gravity center of the aircraft.

Figure 1 shows the three main relative and projection frames.

For the purpose of flight-path control design, it is sufficient to treat only the translational motion of the aircraft. In this context, the aircraft angle of attack α and bank angle ϕ are considered as pseudocontrols inputs, together with the throttle δ_x.

The system describing the point mass aircraft motion in a three-dimensional frame is (a more detailed description can be found in Boiffier [9]):

$$\begin{cases} \dot{x} = v\cos\gamma\cos\chi \\ \dot{y} = v\cos\gamma\sin\chi \\ \dot{h} = v\sin\gamma \\ \dot{v} = \frac{T\cos\alpha - D}{m} - g\sin\gamma \\ \dot{\gamma} = \frac{(L+T\sin\alpha)\cos\phi}{mv} - \frac{g}{v}\cos\gamma \\ \dot{\chi} = \frac{(L+T\sin\alpha)\sin\phi}{mv\cos\gamma} \\ \dot{m} = -\mathrm{TSFC}\times T \end{cases} \tag{1}$$

where T is the thrust force, m is the aircraft mass, $D = qSC_D$ is the drag, g is the gravity acceleration, $L = qSC_L$ is the lift, $q = \frac{1}{2}\rho v^2$ is the dynamic pressure, ρ is the air density, S is the aircraft reference wing area, v is the aircraft aerodynamic speed, γ is the flight-path angle, χ is the heading angle, C_L and C_D are the lift and drag coefficients, and TSFC is the thrust-specific fuel-consumption factor.

For convenience, we define three vectors: $X = (x, y, h, v, \gamma, \chi, m)^T$, $U = (\delta_x, \alpha, \phi)^T$, and p. The first two vectors implicitly depend on time $t \in [t_0, t_f]$ and may be noted by $X(t)$ and $U(t)$. The notation $\dot{x} = dx/dt$ is the first derivative of a component with respect to time. The start time t_0 and end time t_f are assumed constant. Problems with free start or end times can easily be transformed to problems with fixed start and end times. The vector-valued function X: $[t_0, t_f] \to \mathbb{R}^7$ is restricted to be a solution of the nonlinear ordinary differential equation (ODE) in Eq. (1). We call X the state function or state variable, because X describes the state of a dynamical system. Generally, the measurable vector-valued function U: $[t_0, t_f] \to \mathbb{R}^3$ influences the solution of ODE (1) or, in other words, controls the dynamical system. Therefore, we call U the control function. To make a distinction between time-dependent and time-independent optimization variables, the finite dimensional parameter vector p is introduced (p could contain the gravitational acceleration, the wing

Received 27 October 2009; revision received 4 March 2010; accepted for publication 3 May 2010.

*Ph.D. Student, Claude Bernard Lyon 1 University; Transport and Environment Laboratory, 25 Avenue François Miterrand; mohamed.houacine@inrets.fr.

†Researcher, Transport and Environment Laboratory, 25 Avenue François Miterrand; salah.khardi@inrets.fr.

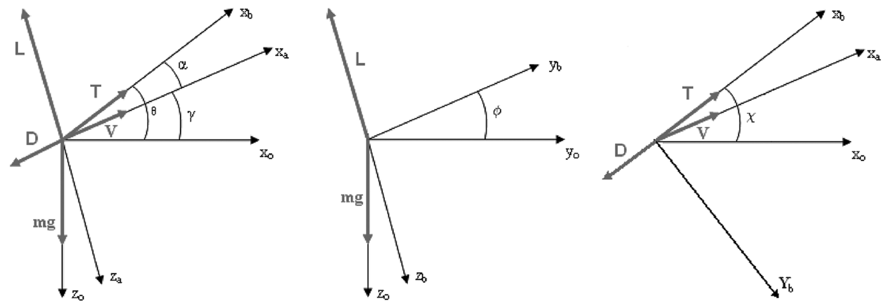

Fig. 1 Body frame $R_b(G, X_b, Y_b, Z_b)$, aerodynamic frame $R_a(G, X_a, Y_a, Z_a)$, and Earth frame $R_0(G_0, X_0, Y_0, Z_0)$.

reference area, etc.). We could equivalently state the optimization problem without p by extending U with components that are constant over time.

Let us denote the dynamic system Eq. (1) by

$$\dot{X} = f(X(t), U(t), t; p) \tag{2}$$

B. Constraints

In addition to the dynamic constraint Eq. (2), we consider two types of constraints we call boundary conditions and path constraints, defined as follows:

With boundary conditions, the flight simulation must start from a feasible fixed initial state $X(t_0)$ and finish at another feasible endpoint $X(t_f)$. Assume that Φ is the function translating these conditions and it takes its values in the interval $[\Phi_{\min}, \Phi_{\max}]$. Then we express the boundary conditions by the following inequalities:

$$\Phi_{\min} \leq \Phi(X(t_0), t_0, X(t_f), t_f; p) \leq \Phi_{\max} \tag{3}$$

With path constraints, state and control variables have to be inside an admissible range of values during the flight. We call this kind of restriction *path constraints*. A simple and general form may be given by

$$C(X(t), U(t), t; p) \leq 0, \qquad \forall\ t \in [t_0, t_f] \tag{4}$$

C. Objectives

Our interest is composed of two subobjectives: 1) to minimize noise under the flight path and 2) to minimize consumed fuel during operations. Several parameters are needed to calculate these two objective functions. We orient the reader to the work of Benson [7] for an explicit description.

1. Noise Function

We consider the noise radiated from the jet exhaust of the engines. We use the well-known Stone model [6], which we recall here:

$$\begin{aligned}\mathrm{OASPL} = 141 + 10\log\left[\left(\frac{\rho}{\rho_{\mathrm{ISA}}}\right)^2\left(\frac{c}{c_{\mathrm{ISA}}}\right)^4\right] + 10\log\left(\frac{A_j}{R^2}\right) \\ + 10\log\left(\frac{\rho_j}{\rho}\right)^{\omega} + 10\log\left(\frac{V_j}{c}\right)^{7.5} - 15\log[(1+M_c\cos\theta)^2 \\ + \beta^2 M_c^2]\end{aligned} \tag{5}$$

This is an OASPL (overall sound pressure level) assessed at a position (R, θ), where R is the distance to the noise source; θ is the angle measured downstream from the jet exhaust axis; ρ and c are, respectively, density of air and speed of sound in the freestream conditions; ρ_{ISA} and c_{ISA} are the air density and the sound velocity in ISA (International Standard Atmosphere) conditions; and A_j, ρ_j, and V_j are fully expanded jet area, jet exhaust density, and jet velocity, respectively. The following analytic expression is used for ω (in [10]):

$$\omega = \frac{3(V_j/c)^{3.5}}{0.6 + (V_j/c)^{3.5}} - 1 \tag{6}$$

This expression gives similar values to those suggested in [11]. The source convection is introduced to translate the effect of directivity in sound radiation. Following Williams [12], the acoustic intensity is multiplied by $[(1 + M_c\cos\theta)^2 + \beta^2 M_c^2]^{-n/2}$, where $M_c = kV_j/c$ is the convective Mach number. In this formulation we took $k = 0.62$ and $n = 3$, as suggested by Goldstein and Howes [13], and $\beta = 0.2$, essentially given by Larson et al. [14]. Refraction corrections are not considered, since no spectral composition is used in this study. So the noise minimization criterion can be expressed by

$$\int_{t_0}^{t_f} J_1(X(t), U(t), t; p)\,\mathrm{d}t = \int_{t_0}^{t_f} \mathrm{OASPL}(X(t), U(t), t; p)\,\mathrm{d}t \tag{7}$$

2. Fuel-Consumption Function

The calculation of the fuel burn in this study is based on the assumptions and equations outlined by Benson [7]. Basically, the instantaneous fuel flow $FF(t)$ can be estimated by

$$FF(t) = \mathrm{TSFC} \times T(t) \tag{8}$$

TSFC is specified as a function of airspeed. So we simply state the second objective function as

$$J_2(X(t_f), t_f; p) = \int_{t_0}^{t_f} -\dot{m}(t)\,\mathrm{d}(t) = [m(t)]_{t_f}^{t_0} = m(t_0) - m(t_f) \tag{9}$$

where $m(t_0)$ and $m(t_f)$ are the initial and final aircraft mass. Since $m(t_0)$ is a constant, in optimization theory we have the following equivalence:

$$\min J_2(X(t_f), t_f; p) \equiv \min -m(t_f)$$

An additive aggregation of J_1 and J_2 is enough for our minimization purpose. We write

$$J(X(t), U(t), t; p) = \int_{t_0}^{t_f} J_1(X(t), U(t), t; p)\,\mathrm{d}t + J_2(X(t_f), t_f; p) \tag{10}$$

which is exactly the Bolza form [15] of the cost function in optimal control theory.

D. Final Form

To summarize, we give the final formulation of our problem. It is a one-phase optimal control problem that consists of a Bolza objective function minimization subject to dynamics, boundary, and path constraints:

$$\begin{cases} \min_{U\in\mathcal{U}} J(X(t),U(t),t;p) = \int_{t_0}^{t_f} J_1(X(t),U(t),t;p)\,\mathrm{d}t + J_2(X(t_f),t_f;p) \\ \dot{X} = f(X(t),U(t),t;p) \\ \Phi_{\min} \le \Phi(X(t_0),t_0,X(t_f),t_f;p) \le \Phi_{\max} \\ C(X(t),U(t),t;p) \le 0 \end{cases} \tag{11}$$

III. Methodology of Resolution

Many methods for solving optimal control problems are described in literature, such as shooting methods [16], collocation methods [17,18], etc. We chose a collocation algorithm called Gauss pseudospectral method (GPM) because of its efficiency in the approximations of three types of mathematical objects: the integration in the cost function, the differential equation of the control system, and the state-control constraints. The GPM for the one-phase control problem Eq. (11) is summarized as follows. First, the original time interval $t \in [t_0, t_f]$ is transformed to the time interval $\tau \in [-1, 1]$ via the affine transformation:

$$t = \frac{(t_f - t_0)\tau + (t_f + t_0)}{2} \tag{12}$$

Using the transformation of Eq. (12), the cost function of Eq. (10) is then given in terms of τ as

$$\begin{aligned} &J(X(\tau),U(\tau),\tau;t_0,t_f;p) \\ &= \frac{t_f - t_0}{2}\int_{-1}^{1} J_1(X(\tau),U(\tau),\tau;t_0,t_f;p)\,\mathrm{d}\tau \\ &+ J_2(X(1),t_f;p) \end{aligned} \tag{13}$$

Similarly, the dynamic constraints of Eq. (2) are given in terms of τ as

$$\frac{\mathrm{d}X}{\mathrm{d}\tau} = \frac{t_f - t_0}{2} f(X(\tau),U(\tau),\tau;t_0,t_f;p) \tag{14}$$

Finally, the boundary conditions of Eq. (3) are given in terms of τ as

$$\Phi_{\min} \le \Phi(X(-1),t_0,X(1),t_f;p) \le \Phi_{\max} \tag{15}$$

and the path constraints of Eq. (4) may be written in terms of τ:

$$C(X(\tau),U(\tau),\tau;t_0,t_f;p) \le 0, \qquad \forall\ \tau \in [-1,1] \tag{16}$$

Suppose now that we approximate the state, $X(\tau)$ in terms of basis of $N+1$ Lagrange interpolating polynomials on the interval $[-1, 1]$ as

$$X(\tau) \approx \tilde{X}(\tau) = \sum_{k=0}^{N} \tilde{X}_k L_k(\tau) \tag{17}$$

where $L_k(\tau)$ $(k = 0, \ldots, N)$ are defined by

$$L_k(\tau) = \prod_{j=0, j\ne k}^{N} \frac{\tau - \tau_j}{\tau_k - \tau_j} \tag{18}$$

and $\tilde{X}_k = \tilde{X}(\tau_k)$. Additionally, the control is approximated using a basis of N Lagrange interpolating polynomials $L_k^*(\tau)$ $(k = 1, \ldots, N)$ as

$$U(\tau) \approx \tilde{U}(\tau) = \sum_{k=1}^{N} \tilde{U}_k L_k^*(\tau) \tag{19}$$

where $L_k^*(\tau)$ $(k = 1, \ldots, N)$ are defined as

$$L_k^*(\tau) = \prod_{j=1, j\ne k}^{N} \frac{\tau - \tau_j}{\tau_k - \tau_j} \tag{20}$$

$\tilde{U}_k = \tilde{U}(\tau_k)$, and τ_k $(k = 0, \ldots, N)$ are the Legendre–Gauss (LG) points that belong to $[-1, 1]$ and are solutions to the Nth-order Legendre polynomial $P_N(\tau)$.

The derivative approximation of the state at the Gauss points is then obtained as

$$\begin{aligned} \left[\frac{\mathrm{d}X}{\mathrm{d}\tau}\right]_{\tau_i} \approx \left[\frac{\mathrm{d}\tilde{X}}{\mathrm{d}\tau}\right]_{\tau_i} &= \sum_{k=0}^{N} \tilde{X}_k \left(\frac{\mathrm{d}L_k}{\mathrm{d}\tau}\right)_{\tau_i} = \sum_{k=0}^{N} D_{ik}\tilde{X}_k \\ &= f(\tilde{X}_i, \tilde{U}_i, \tau_i; p) \end{aligned} \tag{21}$$

where D_{ik} is called the differentiation matrix. It is noted that the differential operators $D \in \mathbb{R}^{N\times N}$ and $\bar{D} \in \mathbb{R}^{N}$ are found using the exact derivative of the Lagrange interpolating polynomials, $L_k(\tau)$ as

$$D_{ik} = \dot{L}_i(\tau_k) = \sum_{l=0}^{N} \frac{\prod_{j=0, j\ne i,l}^{N}(\tau_k - \tau_j)}{\prod_{j=0, j\ne i}^{N}(\tau_i - \tau_j)} \tag{22}$$

The continuous-time optimal control problem is discretized into a nonlinear programming problem (NLP) using variables $\tilde{X}_k \in \mathbb{R}^n$ for the states and $U_k \in \mathbb{R}^m$ for the controls at the LG points $(k = 1, \ldots, N)$. The initial and terminal states $\tilde{X}_0 \equiv \tilde{X}(-1) \in \mathbb{R}^n$ and $\tilde{X}_f \equiv \tilde{X}(1) \in \mathbb{R}^n$ are also included as variables.

First, the continuous-time cost functional of Eq. (13) is approximated using a Gauss quadrature [19] as

$$\begin{aligned} J(\tilde{X}(\tau),\tilde{U}(\tau),\tau;t_0,t_f;p) &= \frac{t_f - t_0}{2}\sum_{k=1}^{N} \mathcal{W}_k J_1(\tilde{X}_k,\tilde{U}_k,\tau_k;t_0,t_f;p) \\ &+ J_2(\tilde{X}_f,t_f;p) \end{aligned} \tag{23}$$

where $\mathcal{W}_k$ are the Gauss weights. Next, the differential equation constraints of Eq. (14) are discretized at the Gauss points as

$$\begin{aligned} \frac{2}{t_f - t_0}\bar{D}_i\tilde{X}(t_0) + \frac{2}{t_f - t_0}\sum_{k=1}^{N} D_{ik}\tilde{X}_k &= f(\tilde{X}_i,\tilde{U}_i,\tau_i;t_0,t_f;p) \\ i &= 1,\ldots,N \end{aligned} \tag{24}$$

where

$$[\bar{D}_i \quad D_{ik}] = \left[\left(\frac{\mathrm{d}L_0}{\mathrm{d}\tau}\right)_{\tau_i} \quad \left(\frac{\mathrm{d}L_k}{\mathrm{d}\tau}\right)_{\tau_i}\right] \in \mathbb{R}^{(N+1)\times(N+1)} \tag{25}$$

It is noted that unlike previously developed pseudospectral methods such as Elnagar and Kazemi [18], in the one developed by Rao et al. [8], the differential equations are collocated only at the LG points and not at the boundary points. Then the discretized boundary conditions are given as

$$\Phi_{\min} \le \Phi(\tilde{X}_0, t_0, \tilde{X}_f, t_f; p) \le \Phi_{\max} \tag{26}$$

Furthermore, the path constraint of Eq. (16) is evaluated at the Gauss points as

Table 1 Aircraft specifications

Type	Airbus A300-600
Powerplants	Two 262.4 kN General Electric CF6-80C2A1s
Weights	Max takeoff 165,900 kg. Operating empty 90,965 kg
Dimensions	Wing span 44.84 m, length 54.08 m, height 16.62 m. Wing area 260 m^2

$$C(\tilde{X}_k, \tilde{U}_k, \tau_k; t_0, t_f; p) \leq 0, \qquad k = 1, \ldots, N \tag{27}$$

Finally, the terminal state $\tilde{X}_f$ is defined using a quadrature approximation to the dynamics as

$$\tilde{X}_f = \tilde{X}_0 + \frac{t_f - t_0}{2} \sum_{k=1}^{N} \mathcal{W}_k f(\tilde{X}_k, \tilde{U}_k, \tau_k; t_0, t_f; p) \tag{28}$$

The cost function of Eq. (23), the constraints of Eqs. (24), (26), and (27) define an NLP. The solution of this NLP is an approximate solution to the continuous-time optimal control problem Eq. (11). The resulting NLP can be solved by an appropriate method taken from the well-known nonlinear programming theory.

IV. Numerical Results and Discussions

In this section we present and discuss some numerical results. The problem is implemented using GPOPS-MATLAB® [20] software and run on an Intel Core2 Quad processor (2.66 GHz, 4 GB memory). Derivatives are approximated by the numerical INTLAB derivation method. The NLP resulting after discretization is solved by SNOPT optimization algorithm [21]. Local optimal solutions are obtained with an average order of feasibility error of 10^{-10}. Units are in the International System. The aircraft model used in the following simulations is described in Table 1.

Practically, we introduce boundary conditions and path constraints for takeoff as follows: the start point is $X(t_0) = (0, 0, 0, 75, 13, 0, 140, 000)^T$, which corresponds to 3-D position$(x(t_0), y(t_0), h(t_0)) = (0, 0, 0)$, takeoff velocity $v(t_0) = 75$ m/s, flight-path angle $\gamma(t_0) = +13°$, heading $\chi(t_0) = 0°$, and initial mass $m(t_0) = 140, 000$ kg. The terminal state is

$$X(t_f) = (\text{free}, \text{free}, 2000, 160, 3, \text{free}, \text{free})^T$$

Time range in seconds is $t_0 = 0$ and $t_f = \text{free} \in [t_{f_{\min}}, t_{f_{\max}}]$. Path constraints are given $\forall\ t \in [t_0, t_f]$ by

$$0.2 \leq \delta_x(t) \leq 1, \qquad -10° \leq \alpha(t) \leq 20°$$
$$-10° \leq \phi(t) \leq 10°, \qquad 0 \leq x(t) \leq 60, 000$$
$$-10000 \leq y(t) \leq 10, 000, \qquad 0 \leq h(t) \leq 2500$$
$$68 \leq v(t) \leq 160, \qquad 0° \leq \gamma(t) \leq 15°, \qquad -10° \leq \chi(t) \leq 10°$$

For landing, the start point is $X(t_0) = (\text{free}, 0, 2000, 110, -5, 0, 125, 000)^T$, which corresponds to 3-D position $(x(t_0), y(t_0), h(t_0)) = (\text{free}, 0, 2000)$, initial velocity $v(t_0) = 110$ m/s, flight-path angle $\gamma(t_0) = -5°$, heading $\chi(t_0) = 0°$, and initial mass $m(t_0) = 125, 000$ kg. The terminal state is $X(t_f) = (0, 0, 0, 65, 0, 0)^T$. Time range in seconds is $t_0 = 0$ and $t_f = \text{free} \in [t_{f_{\min}}, t_{f_{\max}}]$. Path constraints are given $\forall\ t \in [t_0, t_f]$ as

$$0.2 \leq \delta_x(t) \leq .9, \qquad -10° \leq \alpha(t) \leq 20°$$
$$-10° \leq \phi(t) \leq 10° \qquad -60, 000 \leq x(t) \leq 0$$
$$-10, 000 \leq y(t) \leq 10, 000, \qquad 0 \leq h(t) \leq 2500$$
$$63 \leq v(t) \leq 140, \qquad -5° \leq \gamma(t) \leq 2°, \qquad -10° \leq \chi(t) \leq 10°$$

Obtained noise levels and altitude profiles are given in Fig. 2 for both cases of landing and takeoff, with respect to the horizontal distance traveled by the aircraft. This is to highlight the value range of the jet noise assessed at ground level under the flight path.

Figure 3 gives the main obtained results for takeoff. We may observe that the average climbing slope is about 15% (i.e., around $+8.6°$). The throttle is set to its maximum $\delta_x \approx 1$ for the whole flight and the finesse is quite good (around 17). It is important to note that no engine overheating restriction is included in our current model and we assume that the engines can be run in a full power setting over the considered time span. Thrust cutbacks would show up if this restriction was taken into account or if more weight was applied to the fuel cost function.

Figure 4 gives the variation of the main parameters during approach. The average slope rate is near -4% (i.e., $-2.77°$), which is very close to that recommended by ICAO [4]: continuous-descent approach.

The throttle is kept at a low setting to reduce the jet exhaust speed and therefore emitted noise. The finesse is, on average, neighboring 14, which is quite good, because modern aircraft have a finesse between 8 and 20.

In this section, we look for the influence of different optimization criteria. Three cases have been tested: minimizing simultaneously noise and fuel consumption, and noise and fuel separately. We observe that the difference is considerable between the case of optimizing the noise (with or without fuel) and that of minimizing only consumed fuel.

During takeoff (Fig. 5), from 1 to 5 km from brake release, the average noise decrease is around -5.2 dB when we include the noise

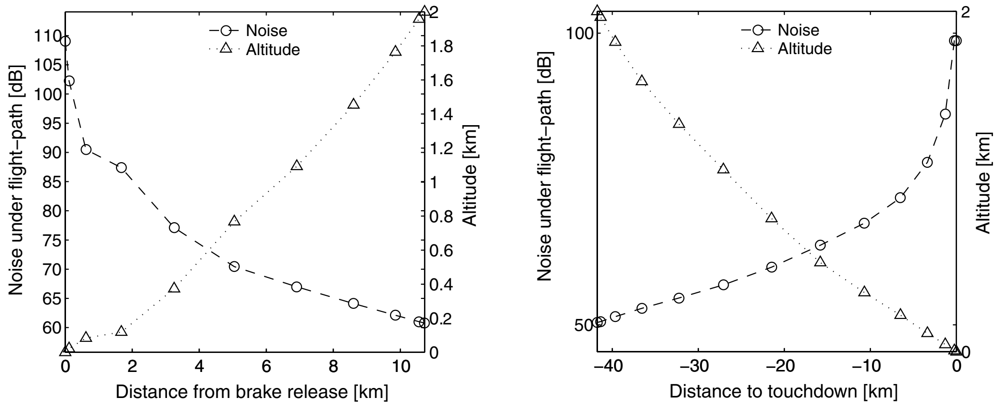

a) Noise levels for takeoff **b) Noise levels for approach**

Fig. 2 Noise levels under flight-path (minimizing fuel and noise).

function in the optimization criterion. This decrease is greater in the first kilometers, which are related to low altitudes. This observation is quite interesting, since the noise concern is more important at low altitudes (high disturbance).

In the approach phase (Fig. 6), we note a quite significant noise reduction when we include noise criterion in the optimization model. From −41.5 to −20 km to touchdown point, the process leads to less than −1 dB compared to the case of minimizing only fuel consumption. Fortunately, in the last 20 km we get more significant decrease: up to −6.3 dB, on average.

Concerning the fuel consumption (Fig. 7) in takeoff, we observe a decrease of −1.9% when we minimize only fuel instead of minimizing noise alone or noise and fuel. If we optimize noise and fuel instead of noise alone, we obtain −0.23%, which is equivalent to −1.27 kg per takeoff (Lyon Saint Exupéry airport: 128,397 movements in 2006 indicates 170 t of fuel reduction). In the approach operations, −2.5% of fuel burn when we minimize only fuel (Lyon Saint Exupéry airport: 128,397 movements in 2006 indicates 362 t of fuel benefit). Figure 7b seems to imply a tradeoff between noise and fuel burn on approach. Continuous-descent approaches are often touted but have never been demonstrated as helpful at reducing both. We note that when we optimize fuel alone, the aircraft airspeed is greater than that obtained when we include noise, and the aircraft therefore takes less time to reach the touchdown point. The airspeed increase is mostly obtained by a decrease in the flight-path angle (thus, the aircraft flight at lower altitudes) and leads to a higher noise impact.

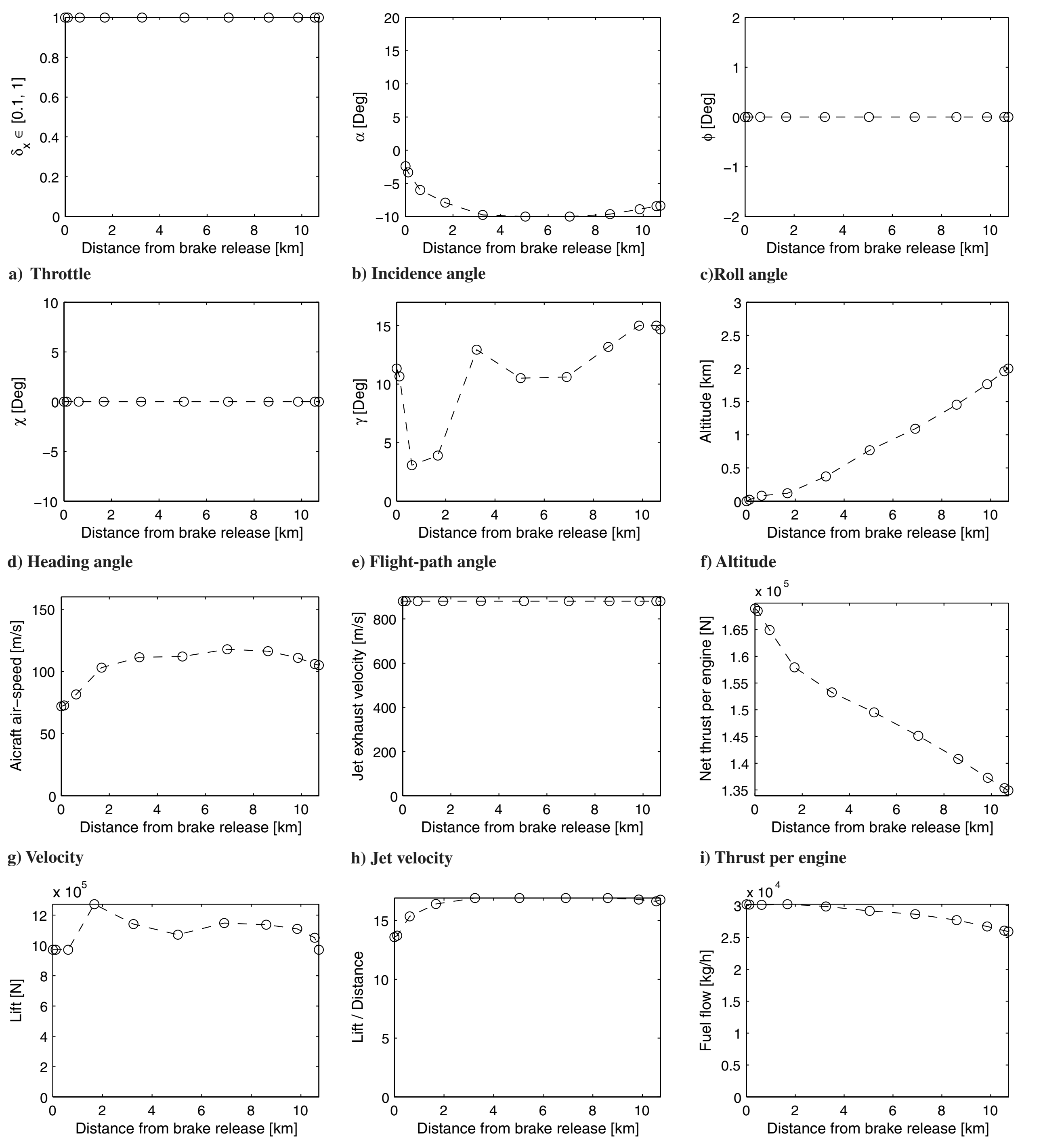

Fig. 3 Optimization results for takeoff (minimizing fuel and noise).

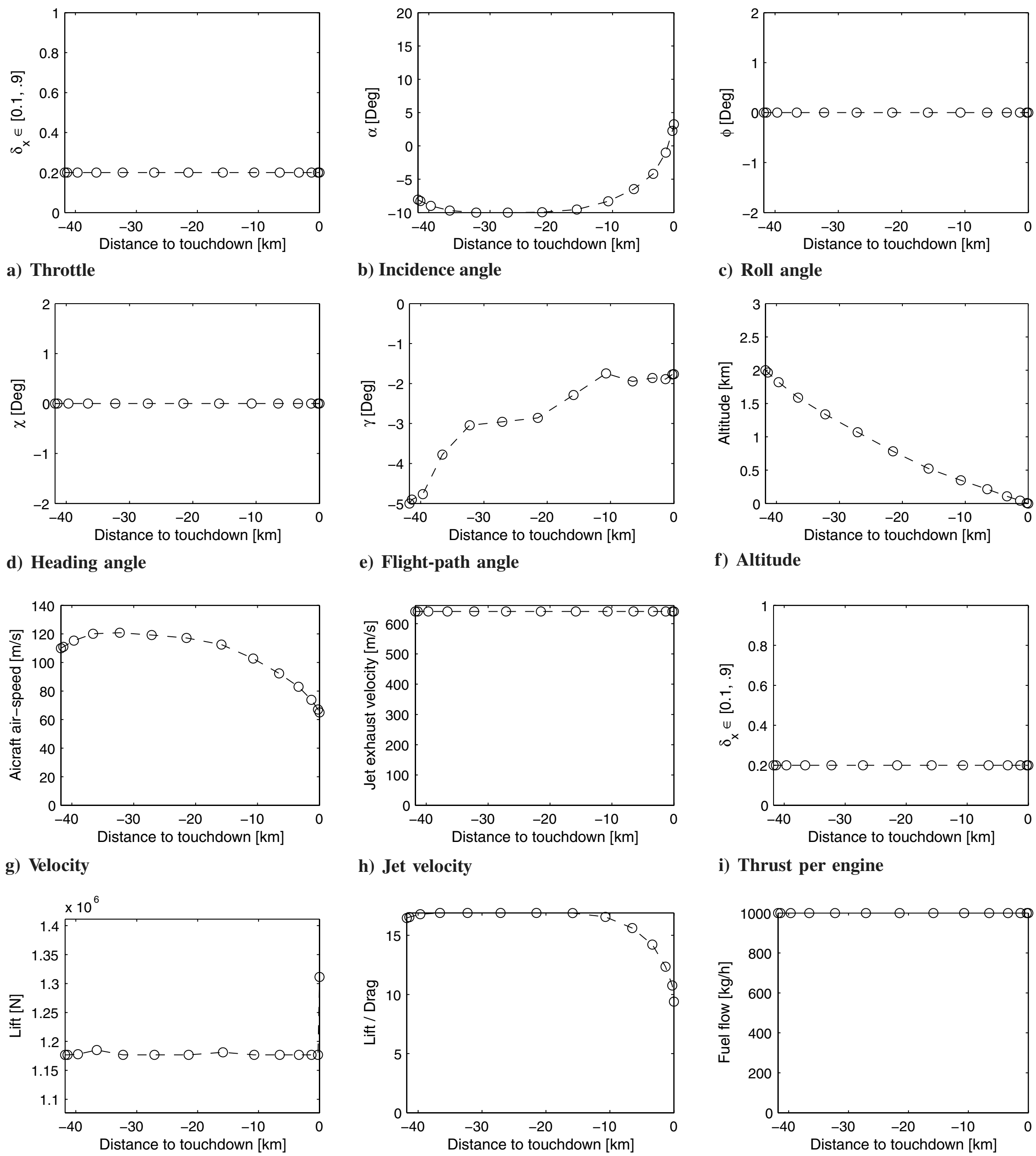

a) Throttle b) Incidence angle c) Roll angle

d) Heading angle e) Flight-path angle f) Altitude

g) Velocity h) Jet velocity i) Thrust per engine

j) Total lift force k) Finesse l) Fuel flow

Fig. 4 Optimization results for landing (minimizing fuel and noise).

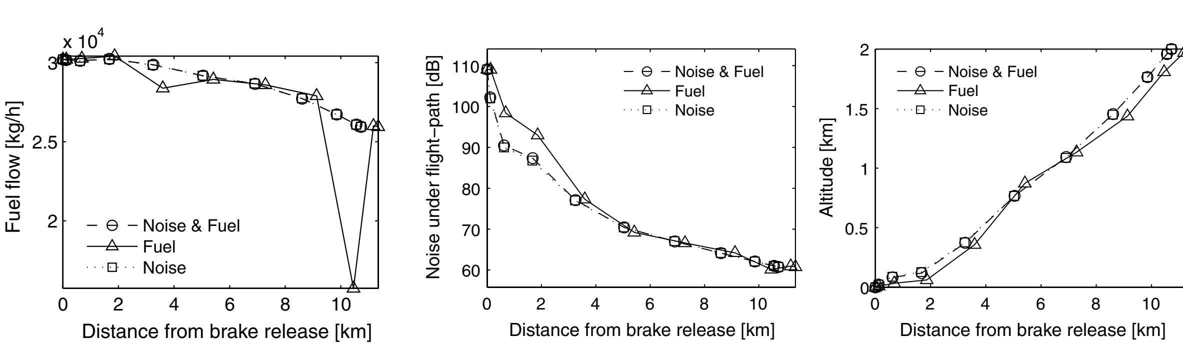

a) Fuel flow b) Noise under flight-path c) Altitude

Fig. 5 Comparison between minimizing: noise and fuel, only noise, and only fuel in takeoff.

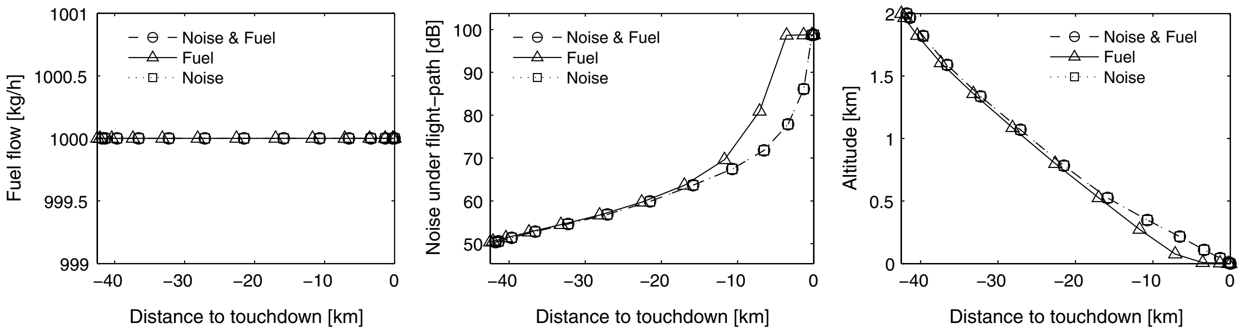

a) Fuel flow **b) Noise under flight-path** **c) Altitude**

Fig. 6 Comparison between minimizing: noise and fuel, only noise, and only fuel in approach.

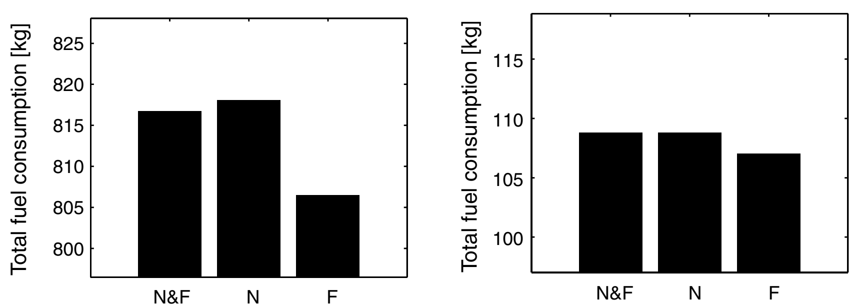

a) Takeoff **b) Approach**

Fig. 7 Total fuel after optimization (N&F: noise and fuel, N: only noise, F: only fuel).

V. Conclusions

To conclude, we have analyzed the benefits of flight trajectory designs that reduce noise and fuel consumption. The problem is addressed as an optimal control problem, which is solved by a Gauss pseudospectral method. Simulation results are given and discussed, and it seems to be that our results are very promising, since for approach, for example, the descent rate is similar to that given by ICAO [4] in order to minimize noise footprints. Our study seems to show a tradeoff between noise and fuel burn on approach. Different conclusions are carried out and some statistical extrapolations are given for Lyon Saint Exupéry International airport to show how fuel consumption (and, consequently, pollutant emissions) can be decreased. It is fundamental to keep in mind that the objective of this research and the expected results are considered to be complementary with technological developments in engine design that aims to increase fuel efficiency and noise control systems innovated by aeronautical manufacturers.

It is obvious that as further research, it will be interesting to incorporate the other noise sources of the aircraft and maybe refine the current fuel-consumption estimation. It will also be interesting to develop an indirect solving method and a dynamic programming application (Bellman optimality principle) to compare with current results.

Acknowledgment

Authors would like to thank La région Rhône-Alpes for the support given in the Cluster de Recherche: Transport, Territoire et Société framework.

References

[1] "Flying by Nature: Global Market Forecast 2007–2026," Airbus France, Toulouse, France, 2007.
[2] "Current Market Outlook 2007," The Boeing Co., Seattle, WA, 2007.
[3] "Noise Standards: Aircraft Type and Airworthiness Certification," Federal Aviation Regulations FAR Part 36, Federal Aviation Administration, June 1974; Consolidated Reprint 12 Aug. 1985.
[4] "Convention on International Civil Aviation," Annex 16, Vol. 1, 3rd ed., International Civil Aviation Organization, Montreal, 1993.
[5] Lilley, G. M., "The Prediction of Airframe Noise and Comparison with Experiment," *Journal of Sound and Vibration*, Vol. 239, 2001, pp. 849–859.
doi:10.1006/jsvi.2000.3219
[6] Stone, J. R., and Montegani, F. J., "An Improved Prediction Method for the Noise Generated in Flight by Circular Jets," NASA TM 81470, 1980.
[7] Benson, T. J., "An Interactive Educational Tool for Turbojet Engines," NASA Lewis Research Center, Cleveland, OH, May 1995.
[8] Rao, A. V., Benson, D. A., Darby, C., Patterson, M. A., Francolin, C., Sanders, I., and Huntington, G. T., "Algorithm 902: GPOPS, A MATLAB Software for Solving Multiple-Phase Optimal Control Problems Using the Gauss Pseudospectral Method," *ACM Transactions on Mathematical Software*, Vol. 37, No. 2, April 2010, Paper 22.
doi:10.1145/1731022.1731032
[9] Boiffier, J.-L., *The Dynamics of Flight*, Wiley, New York, 1998.
[10] Stone, J. R., "Interim Prediction Method for Jet Noise," NASA TM X-71618, 1974.
[11] *Gas Turbine Jet Exhaust Noise Prediction*, Society of Automotive Engineers, Rept. SAE-ARP-876, New York, March 1978.
[12] Williams, J. E. F., "The Noise from Turbulence Convected at High Speed," *Philosophical Transactions of the Royal Society of London, Series A: Mathematical and Physical Sciences*, Vol. 255, 1963, pp. 469–503.
doi:10.1098/rsta.1963.0010
[13] Goldstein, M. E., and Howes, W. L., "New Aspects of Subsonic Jet Noise Theory," NASA TN D-7158, 1973.
[14] Larson, R. S., McColgan, C. J., and Packman, A. B., "Jet Noise Source Modification Due to Forward Flight," AIAA, Paper 77-58, Jan. 1977.
[15] von Andreas Potschka, V., "Handling Path Constraints in a Direct Multiple Shooting Method for Optimal Control Problems," Ph.D. Thesis, Ruprecht-Karls-Universitat, Heidlberg, Germany, May 2006.
[16] Marcelo-Garza, D., "Application of Automatic Differentiation to Trajectory Optimization via Direct Multiple Shooting," Ph.D. Thesis, Univ. of Texas at Austin, Austin, TX, May 2003.
[17] Čižniar, M., Salhi, D., Fikar, M., and Latifi, M. A., "A MATLAB Package for Orthogonal Collocations on Finite Elements in Dynamic Optimisation," *Proceedings of the 15th International Conference*

Process Control '05, edited by J. D. J. Mikleš and M. Fikar, June 2005.
[18] Elnagar, G., and Kazemi, M., "Pseudospectral Chebyshev Optimal Control of Constrained Nonlinear Dynamical Systems," *Computational Optimization and Applications*, Vol. 11, No. 2, 1998, pp. 195–217.
doi:10.1023/A:1018694111831
[19] Davis, P., *Interpolation and Approximation*, Dover, New York, 1975.
[20] Rao, A. V., Benson, D., Huntington, G. T., and Francolin, C., *User's Manual for GPOPS Version 2.2: A MATLAB® Package for Dynamic Optimization Using the Gauss Pseudospectral Method*, Univ. of Florida, Gainesville, FL, Jan. 2010.
[21] Gill, P. E., Murray, W., and Saunders, M. A., "SNOPT: An SQP Algorithm for Large-Scale Constrained Optimization," *SIAM Journal on Optimization*, Vol. 12, 2002, pp. 979–1006.